Neurobiology of Disease 134 (2020) 104645

Contents lists available at ScienceDirect

Neurobiology of Disease

journal homepage: www.elsevier.com/locate/ynbdi

Cerebrospinal fluid neurogranin in an inducible mouse model of neurodegeneration: A translatable marker of synaptic degeneration

Kina Höglund[a,b,c,1], Nathalie Schussler[d,*,1], Hlin Kvartsberg[a], Una Smailovic[e], Gunnar Brinkmalm[a,b], Victor Liman[b], Bruno Becker[a,b], Henrik Zetterberg[a,b,f,g], Angel Cedazo-Minguez[d], Shorena Janelidze[h], Isabel A. Lefevre[d], Stéphanie Eyquem[d], Oskar Hansson[h,i], Kaj Blennow[a,b]

[a] Institute of Neuroscience and Physiology, Department of Psychiatry and Neurochemistry, the Sahlgrenska Academy at the University of Gothenburg, Mölndal, Sweden
[b] Clinical Neurochemistry Laboratory, Sahlgrenska University Hospital, Mölndal, Sweden
[c] Department of Neurobiology, Care Sciences and Society, Center for Alzheimer Disease Research, Neurogeriatrics Division, Karolinska Institutet, Novum, Huddinge, Stockholm, Sweden
[d] Sanofi R&D, Rare & Neurologic Diseases Research Therapeutic Area, Neurodegeneration Research, 1 Avenue Pierre Brossolette, Chilly Mazarin 91380, France
[e] Department of Neurobiology, Care Sciences and Society, Division of Clinical Geriatrics, Karolinska Institutet, Huddinge, Stockholm, Sweden
[f] Department of Neurodegenerative Disease, UCL Institute of Neurology, Queen Square, London, UK
[g] UK Dementia Research Institute at UCL, London, UK
[h] Clinical Memory Research Unit, Lund University, Sweden
[i] Memory Clinic, Skåne University Hospital, Skåne, Sweden

ARTICLE INFO

Keywords:
Neurogranin
SIMOA
CSF biomarker
Alzheimer's disease
Inducible p25 mice
Synaptic loss

ABSTRACT

Synapse impairment is thought to be an early event in Alzheimer's disease (AD); dysfunction and loss of synapses are linked to cognitive symptoms that precede neuronal loss and neurodegeneration. Neurogranin (Ng) is a somatodendritic protein that has been shown to be reduced in brain tissue but increased in the cerebrospinal fluid (CSF) of AD patients compared to age-matched controls. High levels of CSF Ng have been shown to reflect a more rapid AD progression. To gauge the translational value of Ng as a biomarker, we developed a new, highly sensitive, digital enzyme-linked immunosorbent assay (ELISA) on the Simoa platform to measure Ng in both mouse and human CSF. We investigated and confirmed that Ng levels are increased in the CSF of patients with AD compared to controls. In addition, we explored how Ng is altered in the brain and CSF of transgenic mice that display progressive neuronal loss and synaptic degeneration following the induction of p25 overexpression. In this model, we found that Ng levels increased in CSF when neurodegeneration was induced, peaking after 2 weeks, while they decreased in brain. Our data suggest that CSF Ng is a biomarker of synaptic degeneration with translational value.

1. Introduction

Alzheimer's disease (AD) is a progressive neurodegenerative disease with key pathological hallmarks including amyloid plaques, neurofibrillary tangles and neurodegeneration (Scheltens et al., 2016). Loss of synapses is thought to be an early event in the development of AD (DeKosky and Scheff, 1990; Masliah et al., 2001; Scheff et al., 2007) and already at early stages of the disease, dysfunction and loss of synapses are linked to cognitive symptoms and are thought to precede neuronal loss and neurodegeneration (DeKosky and Scheff, 1990; Henstridge et al., 2016). The degree of cognitive impairment has been found to be more closely associated with synaptic loss compared to amyloid plaques or neurofibrillary tangle content (Masliah et al., 2001; Scheff et al., 2007; Blennow et al., 1996; Davies et al., 1987; Sze et al., 1997), particularly in certain areas of the brain, such as the hippocampus (Scheff et al., 2007; Scheff et al., 2006). Consequently, synaptic proteins have the potential to be biomarkers for early AD diagnosis and for monitoring disease progression and effects of disease-modifying therapeutics.

Neurogranin (Ng) is a protein expressed in neurons of the amygdala, hippocampus, cerebral cortex and other associative cortical areas (Bogdanovic et al., 2002). Neurogranin is present in the

* Corresponding author.
E-mail address: nathalie.schussler@sanofi.com (N. Schussler).
[1] The 2 first authors contributed equally to this work.

https://doi.org/10.1016/j.nbd.2019.104645
Received 23 May 2019; Received in revised form 11 October 2019; Accepted 22 October 2019
Available online 25 October 2019
0969-9961/

somatodendritic compartment and can be translocated, upon stimulation, together with calmodulin (CaM) at the dendritic spines where it can sequester CaM, thereby regulating its local availability and controlling the spatiotemporal patterns of Ca2 + /CaM dependent signaling (Diez-Guerra, 2010; Huang and Huang, 2011; Huang et al., 2011; Petersen and Gerges, 2015).

Initial studies demonstrated that levels of Ng were reduced in brain tissue of patients with AD (Davidsson and Blennow, 1998). More recent studies have shown increased levels of Ng in the cerebrospinal fluid (CSF) of patients with AD or with mild cognitive impairment, as compared to healthy controls (Kester et al., 2015; Kvartsberg et al., 2014; Kvartsberg et al., 2015; Thorsell et al., 2010), and high levels have been shown to reflect a more rapid disease progression (Kvartsberg et al., 2014; Mattsson et al., 2016; Portelius et al., 2015). This increase in CSF Ng levels has also been shown to be specific to AD, since it is not observed in other neurodegenerative diseases such as Parkinson's disease, amyotrophic lateral sclerosis and primary tauopathies (Portelius et al., 2018; Wellington et al., 2016). More detailed biochemical studies have shown that Ng is present both as full-length protein and as shorter peptides in brain and CSF; specifically, several C-terminal peptides have been identified (Kvartsberg et al., 2015; Kvartsberg et al., 2018). We have recently demonstrated that Ng in CSF is cleaved in the middle by calpain-1, generating C-terminal peptides that fit with the endogenous peptides described previously (Becker et al., 2018). It is not known today whether this cleavage is linked to disease progression and progressive loss of memory. However, a detailed study of Ng species in brain tissue suggests that cleavage of Ng is upregulated in AD (Kvartsberg et al., 2018).

Translatable pre-clinical models reflecting the pathological spectrum of AD, including amyloid plaques, neurofibrillary tangles and neurodegeneration, are of great value to study disease mechanisms and for drug development. Although several models exist where amyloid plaque and/or tau pathology are present, loss of neurons is rarely part of the described pathology (Hall and Roberson, 2012). Furthermore, a biomarker reflecting events downstream of amyloid and tau pathology and more closely linked to cognition, would be of interest for the development of disease-modifying drugs. There is also a growing consensus that more than one pathological mechanism may need to be addressed to achieve true disease modification in AD; for example an Aβ-targeting drug should potentially be combined with a drug that improves neuronal and/or synaptic health to improve symptoms. Being able to monitor the same biomarker changes in pre-clinical models and in patients would be of great translational value.

To this end, we have developed a highly sensitive immunoassay on the Single molecule array (Simoa) platform for measurement of Ng in CSF from mice and humans. Using this assay, we confirmed an increase in CSF Ng concentration in AD patients compared with cognitively normal controls. We also explored how Ng levels change in the brain and CSF in an inducible transgenic mouse model of neurodegeneration. We used the CamKII-TetOp25 model (referred to as p25 mice) (Cruz et al., 2003), a model in which prolonged p25 expression causes severe synaptic loss and brain atrophy, accompanied by behavioral deficits (Cruz et al., 2003; Fischer et al., 2005). In these mice, we recently described increased CSF levels of neurofilament light (NFL) upon neurodegeneration (Brureau et al., 2017) and in prior studies we also documented substantial synaptic degeneration as demonstrated by reduced levels of the post-synaptic protein PSD-95 in the hippocampus; in contrast, no decrease in hippocampal PSD-95 levels was found in 8 month-old APP/PS1 (Thy1.APPmutxPS1M146L, the mouse model described in Blanchard et al. (Blanchard et al., 2003)), and 9 month-old ThyTau22 (Schindowski et al., 2006) mice compared to wild-type mice (see Supplemental Figs. 1 and 2). The present work aimed to determine whether CSF Ng could be a biomarker of synaptic degeneration with translational value.

2. Material and methods

2.1. Antibodies

The following antibodies were used: the commercially available anti-neurogranin antibody H-6 (Santa Cruz #sc-514922, clone H-6) generated against immunogen 1–50 of Ng, Ng2 which is an in house made monoclonal anti-neurogranin antibody with a suggested epitope of amino acid 52–63 (Kvartsberg et al., 2015) and a rabbit monoclonal anti-Ng antibody (Abcam, ab23570) for Western Blot.

2.1.1. Characterization of the H-6 monoclonal anti-Ng antibody

Western blot (WB) was performed as described previously (Becker et al., 2018). The protocol includes stringent fixation of the transferred proteins and peptides to nitrocellulose by drying the membrane overnight, followed by further fixation by incubation in 0.4% formaldehyde in PBS for 30 min at room temperature.

2.1.2. Epitope mapping by surface plasmon resonance (SPR)-binding measurements

Anti-mouse IgG antibody (mouse antibody capture kit BR-1008-38; GE Healthcare) was immobilized according to kit instructions on a CM5 Biacore chip (BR-1000-12) in a Biacore X100 instrument (GE healthcare, Uppsala, Sweden) *via* amine-coupling at 25 °C in 1× running buffer HBS-EP (BR-1006-69). Using an antibody concentration of 30 μg/mL, a final value of 8770 response units (RU) for the immobilization level was obtained. The cycles for the capture binding analysis were set up as follows: flow rate 10 μL/min; temperature: 25 °C; capture contact time (H-6 antibody at 100 nM in running buffer): 180 s, stabilization period: 180 s; sample contact time (peptide at 300 nM in running buffer): 300 s; dissociation time: 300 s; first regeneration: glycine 10 mM, pH 1.5, contact time 180 s; second regeneration: HCl, 30 mM, contact time 180 s, stabilization period 300 s. The response was measured about 20 s after the end of injection of the peptide ("binding stability") and used to determine the apparent epitope of H-6 (Santa Cruz, sc-514922). Binding analysis was performed using the Biacore X100 Evaluation software (V2.0.1).

2.2. Simoa assay for quantification of mouse and human neurogranin

Capture beads were prepared by conjugation of antibody Ng2 (Kvartsberg et al., 2015) to paramagnetic beads (Quanterix, Lexington, MA, USA) according to the bead supplier's protocol with bead activation at +4 °C with 0.3 mg/mL EDC and antibody conjugation at +4 °C with 0.2 mg/mL antibody. Detection antibody was prepared by biotinylating monoclonal antibody H-6 (Santa Cruz #sc-514922, clone H-6) at a 40-fold molar excess of biotin (Thermo Scientific, 21329) according to the biotin supplier's protocol. Prior to each run, human Ng GST-tagged recombinant protein (produced in house) was serially diluted in 100 mM Tris pH 9.0, 0.05% Tween 20, 0.05% BSA (Assay Diluent). Bead reagent was prepared by inclusion of 70% (n/n) helper beads (Quanterix, Lexington, MA, USA), to conjugated beads. The bead mix was washed and resuspended in Assay Diluent for a total concentration of 20,000 beads/μL. Detection reagent was prepared by dilution of detection antibody to 0.8 μg/mL in Assay Diluent. For each determination, 25 μL bead reagent was mixed with 20 μL detection reagent and 100 μL calibrator or prediluted sample, followed by a 35 min incubation. Afterwards, beads were washed and resuspended in 100 μL streptavidin-conjugated β-galactosidase (Quanterix, Lexington, MA, USA) at 150 pM diluted in SBG Diluent (Quanterix, Lexington, MA, USA). Following 5 min of incubation, the beads were washed and transferred together with resorufin-D-galactopyranoside substrate (Quanterix, Lexington, MA, USA) to an array of wells where each well is sized to accommodate one bead only. The array was imaged to determine individual well light intensities to differentiate between beads with and without bound analyte, giving a signal expressed as average

number of enzymes per bead (AEB). A four-parameter logistic curve fit was applied to the AEB signals corresponding to the known concentrations of the Ng calibrator and sample concentrations were retrieved from the curve based on sample AEBs.

Calibration curve data from five assay runs were used to validate the assay (Andreasson et al., 2015). The Lower Limit of Quantification (LLOQ) was determined by analyzing the deviation from the true value of each calibration point. The deviation for the back-calculated concentrations of the data from the calibrator curve had to be < 25% at LLOQ. The Upper Limit of Quantification (ULOQ) was set to the highest calibrator concentration included and for concentrations between these two limits the deviation for the back-calculated concentrations had to be < 20%. The Limit of Detection (LOD) was determined by adding three standard deviations to the mean AEB of 16 blank measurements and fitting the attained AEB to the calibration curve. Assay precision was validated by repeated measurements of two human CSF samples with different levels of Ng, diluted 8-fold. Precision is reported as the inversely related imprecision measure; the variation coefficient (CV), where repeatability (CV_r) is referred to as the within-run imprecision and (CV_{Rw}) as the intermediate precision. Analysis of variance (one-way ANOVA) was used in the estimation of the imprecision using the formulas in ISO 5725-2.

For the subsequent study runs, calibrators and human CSF control samples were run in duplicates and all samples from each individual patient were measured within the same run. In the pre-clinical studies, mouse CSF was diluted from 24- to 28-fold depending on the smallest amount of individual CSF available, meaning that all samples within one study were analyzed at the same dilution. Brain tissue homogenates from mouse hippocampus were analyzed at 10,000- or 5000-fold dilution. In the clinical study, human CSF was diluted 8-fold.

2.3. Clinical study

Informed consent was obtained for the use of patient clinical data for research purposes.

The AD group (n = 42) consisted of patients fulfilling the criteria for probable AD outlined by the National Institute of Neurological and Communicative Disorders and Stroke and the Alzheimer's Disease and Related Disorders Association (McKhann et al., 1984). The CSF levels of Aβ40, Aβ42 and total tau (t-tau) were analyzed using Euroimmun assays according to the instructions accompanying the kits (Euroimmun, Lübeck, Germany). The IWG-2 criteria were applied (Dubois et al., 2014) using the Aβ42/40 ratio (AD biomarker profile ratio < 0.1 (Janelidze et al., 2016)) and t-tau (AD biomarker profile t-tau > 483 ng/L). The cutoff for t-tau for the Fujirebio assay (400 pg/mL) corresponds to 483 pg/mL for the Euroimmun assay based on data from a published commutability study (Andreasson et al., 2018).

The age-matched control group consisted of cognitively healthy volunteers (n = 50) without history, symptoms or signs of any significant neurological or psychiatric disorder. The study was approved by the Ethical Committee at Lund University (Dnr 2013-494 and 2014-467). Demographic data are presented in Table 1.

2.4. Mouse model for neurodegeneration

All mice in this study were produced and provided by Charles River (Lyon, France). Experiments were performed at Sanofi in an AAALAC-accredited facility in full compliance with standards for the care and use of laboratory animals, according to French and European Community (Directive 2010/63/EU) legislation. All procedures were approved by the local Animal Ethics Committee (CEEA #24) and the French Ministry for Research. Mice were housed in a pathogen-free facility, one per cage, and maintained on a 12-h light/dark cycle with *ad libitum* access to food and water. Mice of both sexes were used (see paragraph 2.9 for more details).

We used an inducible transgenic mouse model overexpressing p25, the CamKII-TetOp25 mice (p25 mice), generated as described by Cruz et al. (Cruz et al., 2003). Briefly, p25 bitransgenic mice were generated using the tetracycline-controlled transactivator system (tTA) to generate bitransgenic mice that inducibly overexpress human p25-GFP under the control of a CamKII promoter, which drives high expression of the p25-GFP transgene in the forebrain. In the presence of doxycycline, a tetracycline derivative, expression of the p25 transgene is repressed. All the mice in this study, including littermate controls, were exposed to doxycycline *in utero* and maintained on a doxycycline containing diet until 6 weeks of age, at which point doxycycline was removed from their diet to induce expression of the human p25-GFP transgene. This event is, hereafter, referred to as induction. XwON refers to bitransgenic animals (p25 mice), whereas WT corresponds to littermate controls that are non-inducible mono-transgenic mice carrying only the TetO-p25 transgene. The very low level of p25 expression in control mice is similar to the level of p25 detected in non-induced p25 mice (data not shown).

Table 1
Demographic data of the clinical study cohort.

	AD	Controls
Number (n)	42	50
Male/Female	13/19	16/24
Age [mean (range)]	74 (53–86)	74 (60–85)
MMSE [mean (range)]	20 (10–27)	29 (28–30)
T-tau (ng/L)	619 (232–1167)	361 (122–1297)
Aβ42/Aβ40 ratio	0.064 (0.031–0.117)	0.117 (0.03–0.178)
Ng (pg/mL) [mean (range)]	2223 (339–6367)	1856 (243–12,270)
Stratifying using the IWG-2 criteria		
Number (n)	28	34
Male/Female	8/20	12/16
Age [mean (range)]	74 (53–85)	76 (60–83)
MMSE [mean (range)]	19 (10–27)	29 (28–30)
T-tau (ng/L)	723 (499–1167)	301 (122–462)
Aβ42/Aβ40 ratio	0.06 (0.03–0.097)	0.13 (0.1–0.18)
Ng (pg/mL) [mean (range)]	2528 (976–6367)	1416 (242–3492)

2.5. Mouse CSF and brain sampling

For CSF sampling, animals were anesthetized with an intraperitoneal injection of a mixture of ketamine hydrochloride (50 mg/kg) and xylasine (10 mg/kg). CSF was sampled, as previously described (DeMattos et al., 2002). Briefly, animals were placed on a platform and the arachnoid membrane covering the cisterna magna was punctured. The positive flow pressure allows collection of CSF using a micropipette with a narrow tip. Five to twenty microliters of CSF per mouse were collected and stored at −80 °C in polypropylene tubes.

Brains were dissected out and the hippocampi were quickly frozen in cooled isopentane and then stored at −80 °C.

2.6. Brain tissue homogenization

Frozen hippocampi were lysed in RIPA buffer (Cell Signaling), containing protease and phosphatase inhibitors (Halt™ Cocktail ThermoScientific), using a Precellys tissue homogenizer and CK14 tubes. After lysis, samples were centrifuged at 14,000 ×g for 10 min at +4 °C. Protein concentrations of the supernatants were determined using DC Protein® Assay (Biorad) and the supernatants were stored at −80 °C pending analyses using Simoa, western blot or immunoprecipitation.

2.7. Western blot (WB) for quantification of neurogranin in mouse brain lysates

Equal amounts of total proteins (10 µg) were submitted to WB analysis with the Novex™ NuPAGE® gel electrophoresis system,

according to the manufacturer's instructions (Life Technologies). Proteins were denatured in LDS buffer containing DTT (70 °C, 10 min) and then loaded onto a NuPAGE® 12% Bis-Tris Mini gel to perform the electrophoresis using MOPS as running buffer (200 V, 50 min). Proteins were then transferred to polyvinylidene difluoridine (PVDF) membranes (0.45 µm, Life Technologies) using X Cell II blot module (30 V for 2 h at RT). Membranes were blocked for 1 h at RT with Tris-buffered saline (TBS)/0.1% Tween 20/5% BSA and incubated overnight at +4 °C with the following primary antibodies: for the evaluation of p25-GFP fusion protein (transgene expression), we used a rabbit polyclonal primary antibody raised against the C-terminal of p25 (C-19) (sc-820, Santa Cruz), and for measuring Ng expression we used a rabbit monoclonal anti-Ng antibody (Abcam, ab23570) which was co-incubated with a rabbit monoclonal anti-GAPDH antibody (Cell Signaling, 2218 L) for normalization of protein loads. The bound antibodies were detected following incubation with an anti-rabbit IgG HRP-conjugated secondary antibody (GE Healthcare, NA940V) for 1 h at room temperature in TBS/0.1% Tween 20/5% non-fat dry milk. Immunoreactive proteins were revealed using a chemiluminescence detection kit (ECL-Select, GE Healthcare). The chemiluminescent signal was captured with a LAS-3000 imaging system (Fujifilm) and densitometry performed with MultiGauge software. To allow quantification across several gels, one sample was used as an internal calibrator and was loaded on each gel and its band intensity set to 100%.

2.8. Immunoprecipitation- mass spectrometry (IP-MS)

Immunoprecipitation (IP) followed by mass spectrometric analyses (MS) was performed as described previously (Kvartsberg et al., 2015). Hippocampal lysates were diluted 40-fold for the IP. Briefly, 8 µg of the Ng2 or H-6 antibodies (Santa Cruz #sc-514,922, clone H-6) were added to 50 µL M-280 Dynabeads (Sheep anti-mouse IgG, Invitrogen) according to the manufacturer's product description and cross-linked as previously described (Brinkmalm et al., 2012). Ng2- or H6-coated beads were used for IP of brain extracts to which Triton X-100 (final concentration 0.05%) was added and incubated at +4 °C overnight. Beads and samples were transferred to a KingFisher magnetic particle processor for automatic washing and elution of full-length and Ng peptides. Eluted Ng was collected and dried in a vacuum centrifuge and re-dissolved in 5 µL 0.1% formic acid (FA)/20% acetonitrile (ACN). Samples were subsequently analyzed using an UltraFleXtreme matrix-assisted laser desorption/ionization time-of-flight/time-of-flight (MALDI TOF/TOF) mass spectrometer (Bruker Daltonics, Bremen, Germany) or high resolution tandem mass spectrometry (MS/MS) using a Dionex Ultimate 3000 nanoflow liquid chromatography (LC) system coupled to a Q Exactive quadrupole–orbitrap mass spectrometer (both Thermo Fisher Scientific). A detailed description about the LC-MS/MS analyses and database searches that were performed can be found in Online Resource 1. All solvents used were of HPLC grade. In both studies in which MALDI TOF/TOF MS was used, the custom Ng peptide RKKIKSGERG-RKGPGPGGPGGAGVARGGAGGGP (corresponding to Ng43–75), with all glycines fully labeled with ^{13}C (theoretical monoisotopic mass: 3010.74 Da; CASLO, Lyngby, Denmark), was added to the tissue homogenate during sample preparation and was used as an internal standard.

2.9. In vivo studies

We first performed a pilot study to establish if levels of Ng were measurable in CSF from induced p25 mice. We included wild type mice (WT, $n = 5$, only male mice) and p25 mice induced for 3 weeks (3wON, n = 5, only male mice). CSF and hippocampal brain tissue were removed at termination. Levels of Ng were measured in mouse CSF (single measure) and brain tissue (duplicate measure) using the Simoa assay. WB was used to assess the levels of full-length Ng in mouse hippocampal lysates.

We then performed a time-course study in p25 mice to evaluate how p25 induction for various time periods affected the CSF levels of Ng. The time periods of induction were chosen according to our previous unpublished data showing the loss of PSD-95 in hippocampus between 2 and 10 weeks (see Supplemental Fig. 1C and 1D). We included mice where p25 was induced for one week (1wON, $n = 13$, 6 male and 7 female), two weeks (2wON, $n = 14$, 6 male and 8 female), four weeks (4wON, n = 14, 6 male and 8 female), and six weeks (6wON, $n = 15$, 7 male and 8 female). In the 6wON group, one male mouse died three weeks after the beginning of induction. At each time point, four wild type mice (WT, 2 male and 2 female) were included. CSF was collected for quantification of Ng using the Simoa assay. Nine samples were excluded due to insufficient CSF volumes.

In the last *in vivo* study, neurodegeneration was induced for four weeks and we included 50 mice in the p25 4wON group (27 male and 23 female) and 49 in the WT group (27 male and 22 female). In this study, both CSF and hippocampi were collected at termination. Ng levels in the soluble fraction of hippocampal lysates were analyzed in all samples both by SIMOA and WB. Besides, 20 of the hippocampal lysates were also used for the characterization of Ng peptides using IP-MS (10 male, 10 female).

2.10. Statistics

Graphs were generated using GraphPad Prism® version 7.02 for Windows (GraphPad Software, San Diego, CA, USA) and statistical analyses were conducted using SAS V9.4 (SAS Institute Inc., USA). Significance level was set at 5%. Since data were not normally distributed and/or with unequal variances, log-transformed data were used for statistical analysis or non-parametric analyses were performed. For the evaluation of Ng in human CSF samples, a Student's test was done on log-transformed data.

In the mouse pilot study, for the evaluation of the Ng levels in CSF or brain tissues, a Wilcoxon-Mann-Whitney test was performed. For the evaluation of the impact of p25 induction on synaptic markers (see Supplemental Fig. 1), a Wilcoxon-Mann-Whitney test was performed followed by a Bonferroni-Holm adjustment. For the time-course study and for the evaluation of four weeks p25 induction (4wON), 2-way ANOVA with factors “sex” and “induction” were performed on log transformed data followed by a Dunnett's multiplicity adjustment in the time-course study. In addition, a Spearman correlation coefficient was calculated on raw data between the levels of Ng measured using Simoa and WB assays.

3. Results

To establish this new assay, we first searched for an antibody combination that could bind to both mouse and human neurogranin. In a previous version of our human Ng ELISA assay (Portelius et al., 2018), anti-Ng antibody Ng2 was combined with Ng22 (epitope 63–75), but the latter did not cross-react with mouse Ng. Therefore, we chose to test the combination of Ng2 as capture and the commercially-available H-6 antibody as detector.

3.1. Characterization of the anti-Ng H-6 antibody

Fig. 1 provides a schematic illustration of Ng, the amino acid sequence in human and the differences with mouse sequence, as well as the suggested epitopes of the antibodies used in the Simoa assay. To identify which Ng species could be detected or immunoprecipitated with the anti-Ng H-6 antibody used for our assay development, we first performed WB and IP-MS analysis (Fig. 2). The WB clearly demonstrated that H-6 could bind to both mouse and human Ng in brain lysates (Fig. 2A) and that it was also able to recognize the human Ng1-42 peptide but not the other forms (Ng9-33, 15-34 and 43-78). IP-MS analysis on mouse brain lysates (Fig. 2B) further demonstrated that H-6

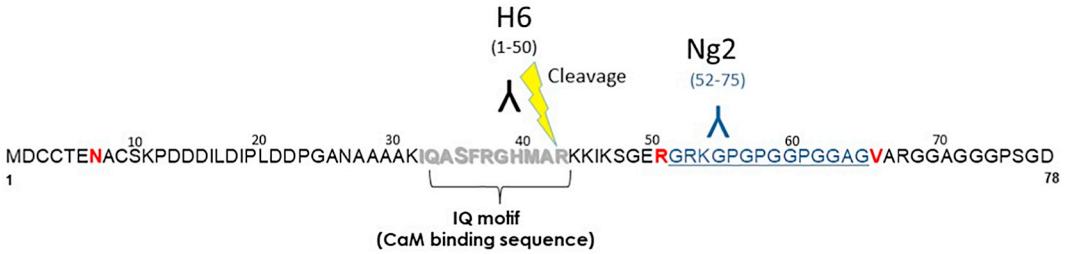

Fig. 1. Schematic illustration of the amino acid sequence of human neurogranin (Ng) where the amino acids which differ compared to mouse Ng are highlighted in red. Monoclonal H-6 antibody is generated by immunizing mice with Ng amino acid 1–50 while Ng2 antibody is generated by using an Ng52-75 peptide. Both antibodies are able to bind human and mouse Ng. The yellow flash illustrates a suggested cleavage of Ng between amino acids 42 and 43. (For interpretation of the references to colour in this figure legend, the reader is referred to the web version of this article.)

could precipitate full-length Ng, while no cleaved Ng peptides were detected (Supplemental Fig. 3). From Table 2, summarizing the responses obtained using the SPR binding measurements, it can be seen that the peptides Ng12-36, Ng40-76 and Ng43-78 did not bind to the H-6 antibody. Therefore, the epitope is likely C-terminal of Ng12-36 and N-terminal of Ng40-76. Indeed, all the peptides that cover that middle region were binding to the H-6 antibody, indicating that amino acids ~37–39 likely is the central epitope for the H-6 antibody (Fig. 1).

Table 2
Summary of the responses recorded when performing epitope mapping of monoclonal anti-neurogranin H6 antibody.

Ng peptide	Binding stability (RU)
Ng12-36	2.6
Ng15-39	23.5
Ng18-42	25.8
Ng24-48	48.3
Ng40-76	−1.2
Ng43-78	1.6

3.2. Simoa assay pre-validation

The calibration range for the Ng assay was set to 0.584–426 pg/mL. The LOD, LLOQ and ULOQ were determined to be 0.92 pg/mL, 1.75 pg/mL and 426 pg/mL respectively, before adjusting for dilutions. In some experiments (Fig. 3 and Fig. 4), an additional upper calibration point was added; all adjusted ULOQs are indicated in the figures and legends. Once adjusted for dilutions and protein levels, neurogranin concentrations were above LOD/LLOQ in all cases, except for a few CSF samples from WT mice. All Ng concentrations in murine samples (CSF or hippocampus homogenates) were below the ULOQ, and all but one human CSF sample contained Ng concentrations below the ULOQ.

At the mean concentration of 24.0 pg/mL of Ng, within-run precision (CV_r) was 7.8% and the between-run precision (CV_{Rw}) was 14%. At a mean concentration of 738 pg/mL, CV_r was 2.8% and CV_{Rw} was 9.2%. Concentrations of precision determinations are adjusted for the 8-fold dilution (validation was performed on human CSF samples 8-fold diluted).

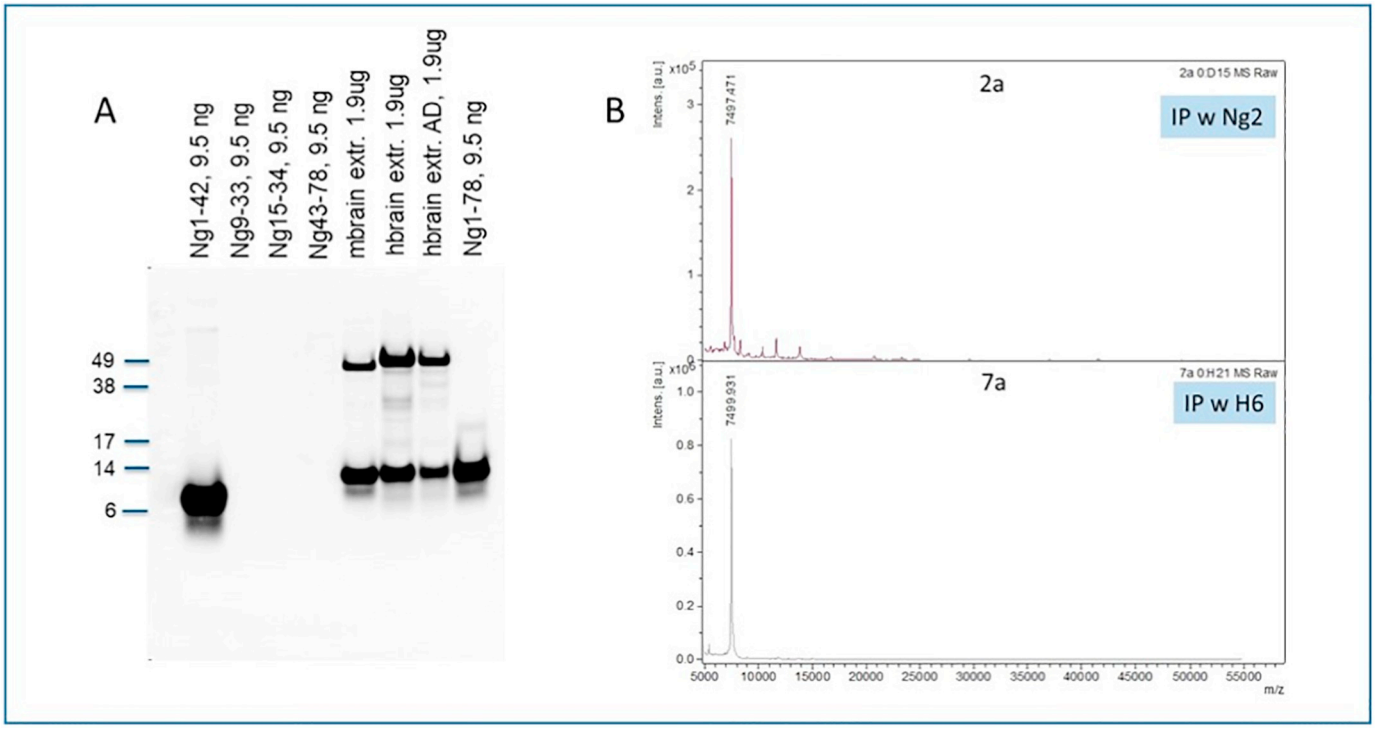

Fig. 2. (A) demonstrates binding of anti-neurogranin H-6 antibody to both mouse and human neurogranin (Ng). Ng peptides 1–42, 9–33, 15–34 and 43–78 contain the human sequence. (B) illustrates the immunoprecipitation of Ng from mouse brain tissue using H-6 or Ng2 monoclonal antibodies coupled to magnetic beads followed by MALDI TOF MS analysis. The theoretical average mass of full length mouse neurogranin (protonated) is 7497.4 Da.

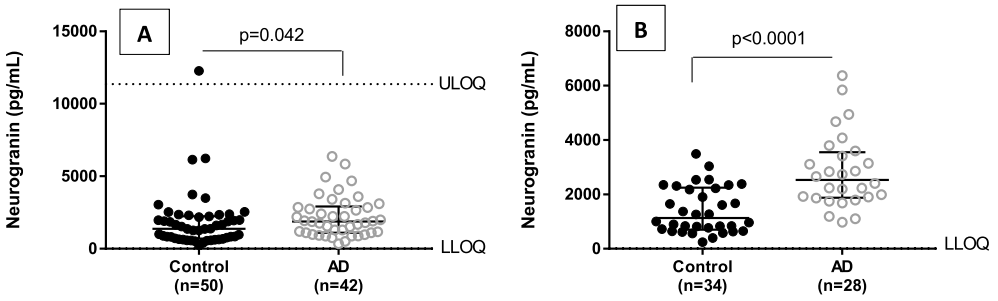

Fig. 3. illustrates the group differences of cerebrospinal fluid levels of neurogranin of the whole cohort (A) and after the exclusion of individuals where clinical diagnosis did not match the biomarker profile (AD criteria: Aβ42/40 ratio < 0.1 and t-tau > 483 pg/mL) (B). Data are presented as median (interquartile range). Adjusted LOD (7.36 pg/mL), LLOQ (14 pg/mL) and ULOQ (11,360 pg/mL) are indicated as dotted lines.
NB: For the calculation of adjusted values for these human CSF samples, the 8-fold dilution was used. And for the adjusted ULOQ, we used the upper calibration point that was run in parallel: 1420 pg/mL (adjusted ULOQ = 1420 × 8 = 11,360 pg/mL).

3.3. Clinical study

We first wanted to evaluate if CSF Ng levels, analyzed with our newly developed Simoa assay which can measure both human and mouse Ng, could still discriminate between patients with AD and healthy controls as previously reported (Kester et al., 2015; Kvartsberg et al., 2014; Kvartsberg et al., 2015). In the whole cohort (healthy controls, $n = 50$ and AD, $n = 42$), the CSF levels of Ng were significantly increased by 36% in patients with AD compared to controls ($p = 0.042$, Fig. 3A). When applying the IWG-2 criteria (AD biomarker profile Aβ42/40 ratio < 0.1 and t-tau > 483), the increase in patients with AD became more evident (121%, $p < 0.0001$, Fig. 3B). For this second analysis, 15 healthy control samples were excluded due to signs of either Aβ pathology (Aβ42/40 < 0.1) or tau pathology (t-tau > 483) and 1 sample was excluded due to missing values for Aβ and tau. In the AD group, 14 samples were excluded based on the cut-offs (Aβ42/40 > 0.1 or t-tau < 483).

3.4. Mouse studies

3.4.1. Pilot study

In order to validate CSF Ng as biomarker for synaptic degeneration and to validate the new Simoa assay on mouse samples, we used the inducible p25 mouse model. In this model, by measuring the expression of p25-GFP fusion protein in brain tissue by WB, we have already demonstrated that transgene expression is highly induced as early as two weeks after the onset of induction in both cortex (Brureau et al., 2017) and hippocampus (Supplemental Fig. 1A and 1B). In the latter, we also evaluated the impact of p25 induction on synaptic markers in hippocampal lysates and we demonstrated a reduction of PSD-95 of 9–10% after two weeks induction and of 28–38% after five weeks induction (Supplemental Fig. 1C and 1D).

Here, we were able to quantify mouse Ng in hippocampal lysates and CSF. In CSF, all samples were found to be measurable, *i.e.*, above the LOD (Fig. 4A). There was a significant increase (29-fold, $p = 0.008$)

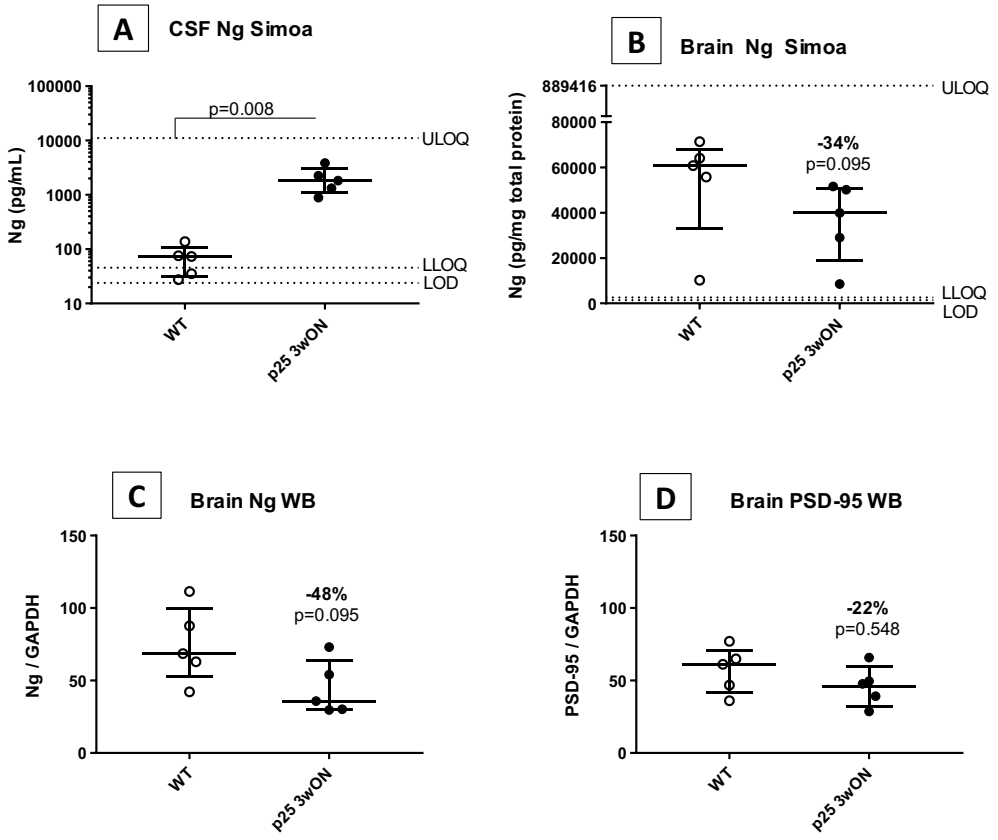

Fig. 4. Panel A illustrates the significant increase in cerebrospinal fluid (CSF) levels of neurogranin (Ng) after three weeks of p25 induction (p25 3wON) compared to wild type mice (WT) (logarithmic scale on Y-axis). Panels B and C illustrate the levels of Ng measured by Simoa and western blot (WB), respectively, normalized against total protein concentration or GAPDH, in the soluble fraction of the hippocampus. There is a non-significant 34% reduction in hippocampus soluble fraction as measured by the Simoa (B) and a non-significant 48% reduction in hippocampus soluble fraction as measured by WB (C). Panel D illustrates the levels of PSD-95, another synaptic protein, in hippocampus of the same mice. The reduction is only of 22%. Data are presented as median (interquartile range). Adjusted LOD, LLOQ and ULOQ are indicated as dotted line. Male mice only.
NB: For the calculation of adjusted values in pg/mg in brain, the 10,000-fold dilution and the mean of total protein concentrations in brain lysates (6.746 µg proteins/µL) were used. For these samples, the upper calibration point run in parallel was 600 pg/mL (adjusted ULOQ = 600 × 10,000/6.746 = 889,416 pg/mg prot.)

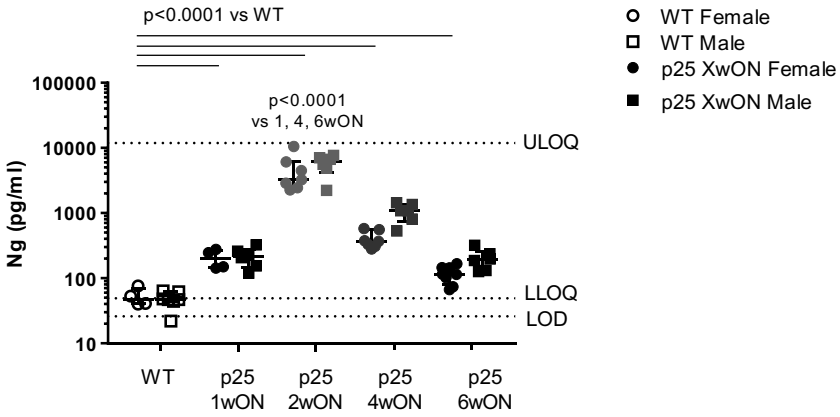

Fig. 5. illustrates the significant increase in neurogranin (Ng) in cerebrospinal fluid (CSF) after one, two, four and six weeks of induction ($p < .001$) compared to wild type (WT) mice. There was also a significant increase in Ng CSF levels after two weeks induction compared to one, four and six weeks induction ($p < .0001$). After six weeks, Ng levels remained still higher than in WT animals. Data are presented as median (interquartile range). Male and female mice. Adjusted LOD (26 pg/mL), LLOQ (49 pg/mL) and ULOQ (11,928 pg/mL) are indicated as dotted line.
NB: for these mouse CSF samples, the 28 -fold dilution was used to calculate the adjusted values and the upper calibration point run in parallel was 426 pg/mL (adjusted ULOQ = 426 × 28 = 11,928 pg/mL).

of Ng after three weeks of p25 induction. In the soluble fraction of hippocampal lysates, levels of Ng measured by Simoa (Fig. 4B) and WB (Fig. 4C) were found to be decreased by 34% and 48%, respectively. This decrease was, however, not statistically significant ($p = 0.095$) on this small number of animals ($n = 5$). In the same brain samples, PSD-95 was only reduced by 22% ($p = 0.548$) (Fig. 4D).

3.4.2. Time-course study

Next, we performed a time-course study in p25 mice with CSF sampling after different time points, one, two, four and six weeks of induction. Samples from the following number of animals were included in the final study $n = 10$ (WT), $n = 11$ (1wON), $n = 13$ (2wON), n = 13 (4wON) and $n = 14$ (6wON). All samples showed Ng concentrations above the LOD except for one sample of the WT group. CSF Ng levels were significantly increased in the p25 mice following induction at all time points tested ($p < 0.0001$ *versus* WT). The highest CSF Ng levels were reached after 2 weeks of induction (6129 pg/mL in male and 3244 pg/mL in female mice). From 2 to 6 weeks, there was a progressive decline in Ng levels reaching 192 and 114 pg/mL at 6 weeks in male and female mice respectively. These levels in the 6wON group still remained higher than the basal levels in the WT group (47 pg/mL) (Fig. 5).

We performed an additional study with p25 4wON mice. We wanted first to characterize Ng peptides in the pool of CSF samples using IP-LC-MS analysis, but we failed to detect enough Ng to be conclusive. The second objective of this study was to evaluate and characterize Ng levels in brain samples. Levels of Ng in hippocampal lysates from p25 4wON ($n = 50$, 23 female, 27 male) and WT mice ($n = 49$, 22 female, 27 male) were analyzed using both Simoa (Fig. 6A) and WB (Fig. 6B and Supplemental Fig. 4). The ~8–9 kDa Ng immunoreactive band corresponding to full length Ng (Supplemental Figs. 4 and 5) was quantified by WB. Ng levels were found to be significantly decreased after four weeks induction, 55% and 38%, for Simoa and WB, respectively ($p < 0.0001$). There was a significant correlation between WB and Simoa quantification (Fig. 6C, $r_s = 0.631$, $p < 0.0001$).

Using IP-MALDI on hippocampal lysates, we identified a total of six Ng peptides. Quantification of these peptides revealed that there was a significant reduction of peptide Ng52-78 (Fig. 7D) in p25 4wON mice compared to WT ($p = 0.0047$). In contrast, no significant differences were found in the quantity of peptides Ng52-72/Ng53-73 (Fig. 7A), Ng53-75 (Fig. 7B), Ng53-78 (Fig. 7C) or Ng43-78 (Fig. 7E), between WT and p25 4wON mice. We verified the identity of three peptides (52-78, 53-75, 53-78) using LC-MS/MS.

4. Discussion

We present a successfully developed and pre-validated ultra-sensitive assay for the quantification of Ng in both mouse and human CSF and we first confirmed that CSF levels of Ng are significantly increased in patients with AD compared to controls, as has been reported previously (Kester et al., 2015; Kvartsberg et al., 2014; Kvartsberg et al., 2015; Thorsell et al., 2010; Wellington et al., 2016). Next, in a small pilot study in p25 mice, we demonstrate that the Simoa assay is sensitive enough for the quantification in CSF from mice with a LOD of 26 pg/mL once adjusted for dilution. Our pilot data also suggest that this mouse model presents a marked increase in CSF Ng upon induction of p25 expression. Furthermore, we show that levels of Ng are concomitantly reduced in the hippocampus of this mouse model using both the Simoa assay and WB. A time-course follow-up study further confirmed that Ng levels in CSF increase upon the induced neurodegeneration, with the maximum increase evidenced after two weeks of induction. In the same model, we report a reduction of PSD-95 in brain after p25 induction. These results are consistent with previous studies in AD patients showing reduction of synaptic proteins in frontal cortex and hippocampus (Diez-Guerra, 2010) and an elevation of Ng in CSF (Davidsson and Blennow, 1998).

In the 4wON study, we have documented a sex difference that could suggest that male mice may be more vulnerable to p25 expression. However, we previously reported that, in this model, the levels of transgene expression, as measured by p25-GFP protein expression, were higher in male mice than in female mice, which also resulted in differential levels of NFL in CSF (Brureau et al., 2017). Thus, it is likely that differences in Ng were also related to differences in p25 expression rather than sex-related.

It is interesting to note that, in our preliminary study, we showed that PSD-95 was decreased in brain tissue after p25 induction. Similar to Ng, PSD-95 is a post-synaptic protein, found in the dendritic spines in the post-synaptic density (Okabe, 2007). There is only a limited number of studies investigating the protein levels of PSD-95 in aging, AD or AD models, and data are contradictory depending on the brain region studied or on the pre-clinical model that was used (Savioz et al., 2014). In the p25 mouse model, the major reduction in PSD-95 was observed after five weeks of p25 induction, suggesting that the effect on PSD-95 is less pronounced and appears later than the effects seen on Ng. As suggested by Savioz et al., this might be because of the dual role of PSD-95, which is involved in both reactive and/or compensatory mechanisms (Savioz et al., 2014).

Included in this study was also the epitope mapping of the monoclonal H-6 antibody which was generated by immunization with Ng amino acid 1–50. Our data suggest that the H-6 antibody has an epitope in the region of amino acids 37 and 39. Interestingly, this sequence (FRG) is part of the IQ-motif (amino acids 33–46 in Ng) which is also found in GAP-43, a neuronal marker. In our study, the H-6 antibody also detects in WB a band of the same apparent molecular weight (around 43 kDa) in human and mouse brain extract, similar to that seen with the GAP-43 antibody NM-4 (Mercken et al., 1992). Cross-reactivity for GAP-43 in our Simoa assay was therefore investigated by spiking GAP-43 at different concentrations into CSF and there were no signs of

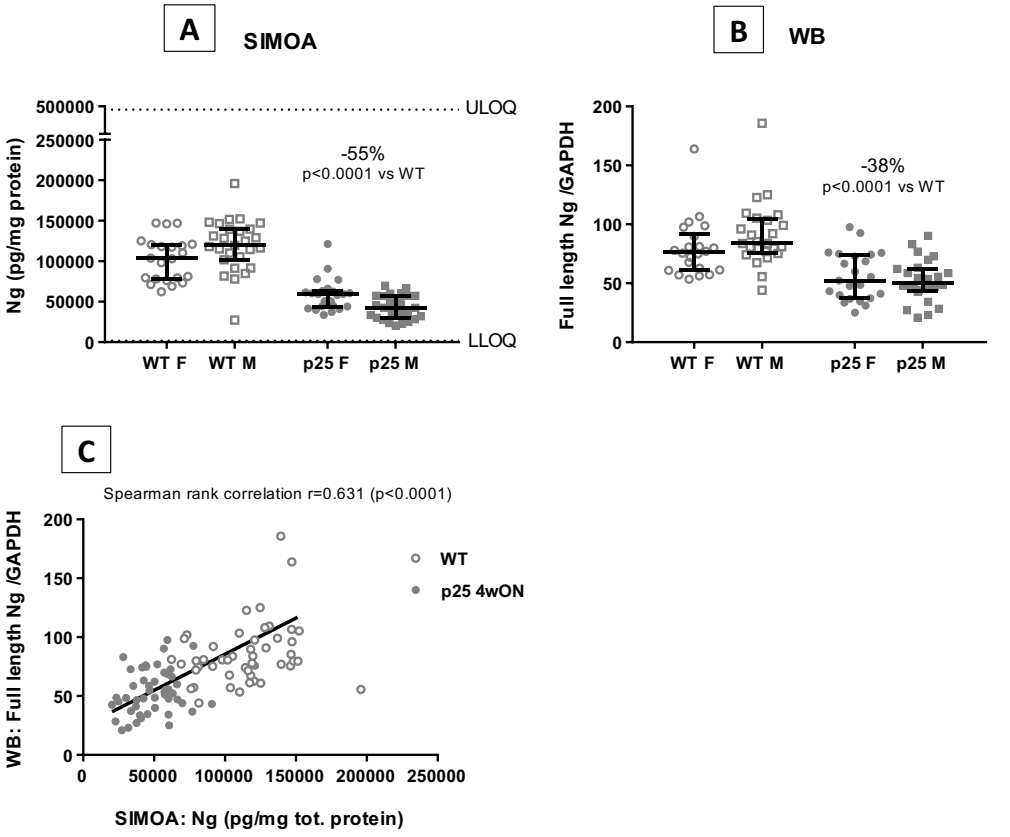

Fig. 6. It displays the levels of neurogranin (Ng) in hippocampal brain tissue from wild type mice (WT) and p25 mice induced for four weeks (p25 4wON) analyzed with the Simoa assay (A) and by western blot (B). There is a significant decrease in Ng after four weeks induction measured both by Simoa and WB. Panel C shows the correlation between Simoa and western blot methods. Data are presented as median (interquartile range). The regression line in Panel C is only for visualization. Adjusted ULOQ and LLOQ for Simoa are indicated as dotted line.
NB: For the calculation in pg/mg, the 5000-fold dilution and the mean of total protein concentrations (4.519 μg proteins/μL) were used. The upper calibration point run in parallel was 426 pg/mL (adjusted ULOQ = 426 × 5,000/
4.519 = 471,473 pg/mg prot.)

cross reactivity. Because the H-6 antibody has been raised against the peptide Ng1-50, it cannot be ruled out that there may be additional epitopes along the sequence Ng1-11 that we did not test in our SPR binding study. Furthermore, an inherent limitation of the epitope-mapping using a set of shorter peptides is that conformational epitopes may not be detectable.

With respect to the many species of Ng found in CSF (Kvartsberg et al., 2015) we also wanted to understand whether the Simoa assay

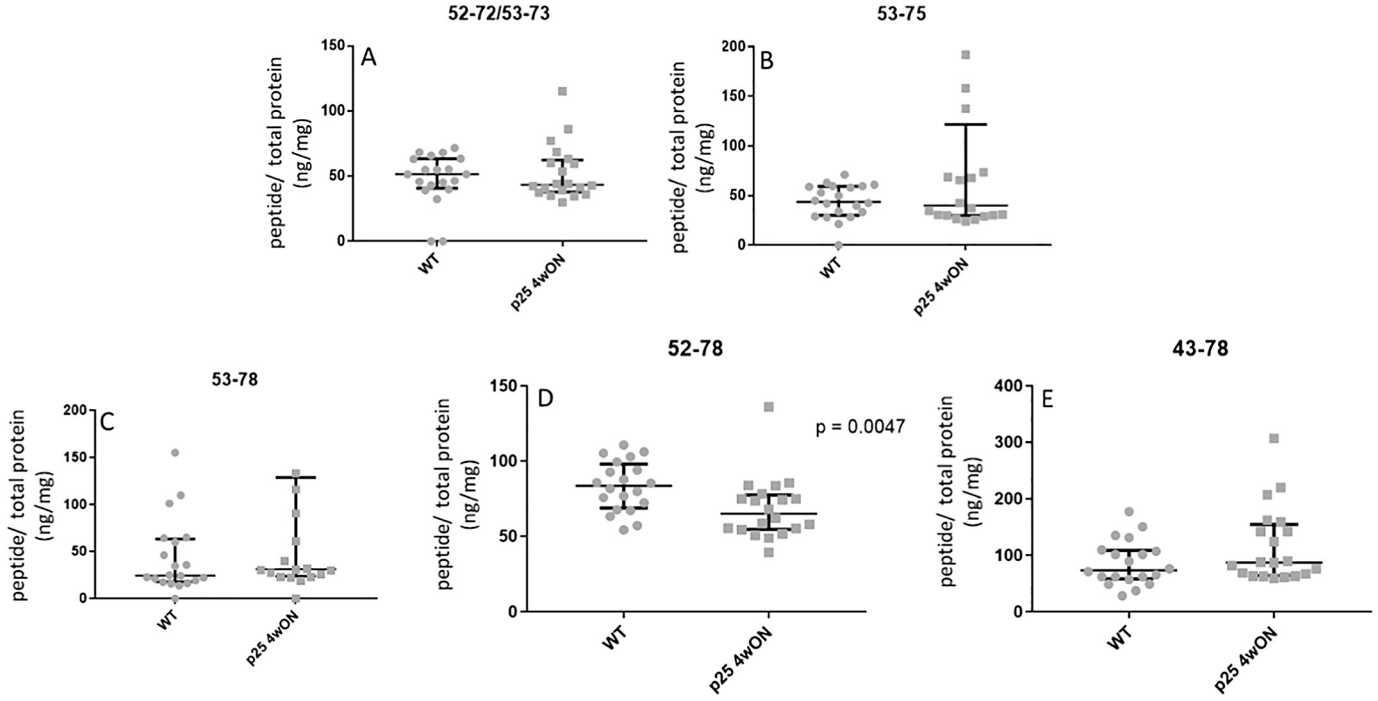

Fig. 7. Panels A-E present the levels of six different neurogranin (Ng) peptides in the soluble hippocampi brain tissue fraction comparing WT (n = 10) and p25 4wON (n = 10). Only peptide Ng52–78 was found to be significantly different comparing WT and p25 4wON (p = .0047). Immunoprecipitation was performed using Ng2 antibody and the identity of the peptides was confirmed using LC-MS/MS.

was measuring full-length Ng (*i.e.*, Ng not cleaved in the middle region) or if it is an assay that measures "total" Ng (*i.e.*, peptides and full-length protein containing the epitopes of the antibodies). As described above, H-6 antibody is believed to bind close to the region where calpain-1 has been shown to cleave (Becker et al., 2018) and our IP-MS data suggest that H-6 antibody only pulls out full-length Ng, indirectly suggesting that the Simoa assay measures full-length Ng. In support of this is the correlation between the WB analyses, which measured full-length protein, and the Simoa analyses. If cleavage of Ng is upregulated in AD, one could speculate that analyzing full-length protein would be a better biomarker than analyzing all species of Ng together ("total"). However, a recent systematic investigation demonstrated that the diagnostic utility of Ng was not assay dependent (Willemse et al., 2018).

Originally generated to explore the role of deregulated brain Cdk5 activity in triggering *in vivo* neurodegeneration, p25 mice display changes in several neurodegenerative mechanisms, including neuronal cytoskeletal alterations, abnormal protein hyperphosphorylation, synaptic dysfunction, cell cycle activation, DNA damage and activation of glial cells (Cruz et al., 2003; Fischer et al., 2005; Kim et al., 2008; Sundaram et al., 2012; Fischer et al., 2007). The ability to regulate the neurodegeneration phenotype in p25 mice makes this a relevant model to evaluate candidate dynamic biomarkers of neurodegenerative processes in biofluids. We have previously characterized the p25 mice model with respect to CSF levels of NFL (Kvartsberg et al., 2018), a protein particularly abundant in axons and associated with neuronal death and axonal degeneration in several neurodegenerative diseases including AD (Rosengren et al., 1996; Skillback et al., 2014). Interestingly, in comparison to CSF NFL levels which correlate with ongoing neurodegeneration in the p25 mice model and peak after four/five weeks (Brureau et al., 2017), our new data demonstrate that Ng levels in mouse CSF reach a maximum after only two weeks of p25 induction. This temporal pattern of changes in CSF suggests that synapse loss precedes neuronal loss in this mouse model, as previously demonstrated in patients with AD (Arendt, 2009; Serrano-Pozo et al., 2012). An alternative interpretation is that p25 induction may have a direct effect on Ng homeostasis by influencing its binding to calmodulin, *e.g.*, by Cdk5 activation (Diez-Guerra, 2010; Huber et al., 2013). In any case, these data further strengthen the utility of this mouse model in time-course biomarker studies and suggest that Ng in CSF could be an earlier biomarker of ongoing neurodegeneration than NFL.

Our next objective was to check if, as we have previously reported in human CSF (Mercken et al., 1992), neurogranin was only detectable as a short C-terminal fragment in mouse CSF and not as full length Ng. But we failed to detect sufficient amounts of Ng peptides to be conclusive.

In human cortex (Mercken et al., 1992), in contrast to CSF, we have reported the detection of several peaks in the mass range of full length Ng corresponding to post-translationally modified Ng and, in addition, several peaks corresponding to short C-terminal peptide species. We have also recently shown that the ratio between some of these C-terminal peptides and full length neurogranin was increased in AD brain (Kvartsberg et al., 2018). We therefore decided to explore whether, in our mouse model of inducible neurodegeneration, C-terminal peptides were also detected and increased in the brain. We identified a total of six C-terminal peptides in the hippocampal lysates of 4wON p25 mice and WT mice. Only one peptide, Ng52–78, was significantly downregulated upon induction. The decrease observed for this peptide, together with the increase in full length Ng contrasted with our previous results obtained in human cortex, as well as with the results of our WB and Simoa analysis in the same hippocampal lysates. This result contrasts also with our preliminary WB analysis, in which we identified in the 2 hippocampal lysates that were analyzed, a short fragment that seems to be increased upon p25 induction together with the reduction of full-length Ng (Supplemental Fig. 5). This short fragment could correspond to the cleavage product we observed after calpain 1 digestion of Ng (Becker et al., 2018). Additional work using both WB and high resolution MS could contribute to further understanding of these findings. The identification of such a cleavage in hippocampus in this model of inducible neurodegeneration would certainly add some translational value to this preclinical model, but this was not the primary objective of our study.

There are two main limitations of the present study.

First, aiming to identify a translational biomarker that could be used to assess the effects of compounds both in animal models and in humans, we have compared observations in AD patients with observations in an inducible p25 mouse model. These mice may not be the first choice of model to study AD like pathology, even if several publications have provided evidence of aberrant APP processing and tau pathology in this model (Cruz et al., 2003; Cruz et al., 2006; Giusti-Rodriguez et al., 2011). But we chose to evaluate CSF neurogranin in this particular mouse model because impairment in learning and memory, as well as synaptic deficits had been documented in these mice after prolonged p25 expression (6wON) in the literature (Fischer et al., 2005; Giusti-Rodriguez et al., 2011) and because we had also observed, in these mice, a substantial reduction of post-synaptic protein PSD-95 levels in two prior studies after 5wON. In contrast, using two other transgenic mouse models of tau or amyloid pathology, the ThyTau22 and APP/PS1 strains, we found that PSD-95 levels were not consistently lower in hippocampus of these mice at 9 and 8 months respectively, when hallmarks of AD pathology are evident. And, when examining potential biomarkers in both nonclinical and clinical studies, we would argue that a focused mechanism-based perspective could serve, since none of the existing mouse models fully recapitulates all the AD pathological hallmarks.

The second limitation of this study is the lack of MCI stages in our small cohort. Several papers support that CSF levels of neurogranin reflect the intensity of synaptic degeneration in AD, and signals in the early stages of the disease. In the early MCI stage of AD, high CSF levels of neurogranin predict future rate of cognitive decline (Kvartsberg et al., 2015; Mattsson et al., 2016; Portelius et al., 2015) and also correlate with future rate of hippocampal atrophy and rate of metabolic reductions on cortical glucose (FDG-PET), especially in amyloid PET positive cases (Mattsson et al., 2016; Portelius et al., 2015). Nevertheless, the aim of the present study was essentially to validate, by confirming previous results obtained in CSF AD samples, the newly developed sensitive Simoa assay which cross-reacts with both mouse and human, thereby supporting translatability.

To conclude, our time-course evaluation of Ng in brain and CSF in the inducible p25 mouse model demonstrates that this pre-clinical model presents similar biomarker signs of synaptic alterations as those seen in patients with AD. Furthermore, our data suggest that Ng is a translatable biomarker of value for future pre-clinical and clinical studies and that it could be an earlier marker than NFL in neurodegenerative diseases. Other mouse models perhaps more relevant of Alzheimer pathology should now be explored with our new Simoa assay. Future studies on CSF levels of Ng and their correlation with behavioral and cognitive changes in mouse models, together with the ongoing longitudinal clinical trials enrolling patients with early symptomatic AD will certainly shed light on the relationship between CSF neurogranin and other CSF biomarkers and cognitive parameters.

Declaration of Competing Interest

N.·S, A.C-M, I.A.L and S.E were employees of Sanofi when the work was performed. H.Z has served at advisory boards for Roche Diagnostics, Wave, CogRx and Samumed, has given lectures in symposia sponsored by Biogen and Alzecure, and is a co-founder of Brain Biomarker Solutions in Gothenburg AB, a GU Ventures-based platform company at the University of Gothenburg. K·B has served as a consultant or at advisory boards for Alzheon, BioArctic, Biogen, Eli Lilly, Fujirebio Europe, IBL International, Merck, Novartis, Pfizer, and Roche Diagnostics, and is a co-founder of Brain Biomarker Solutions in

Gothenburg AB, a GU Ventures-based platform company at the University of Gothenburg. O·H has acquired research support (for the institution) from Roche, GE Healthcare, Biogen, AVID Radiopharmaceuticals, Fujirebio, and Euroimmun. In the past 2 years, he has received consultancy/speaker fees (paid to the institution) from Lilly, Roche, and Fujirebio. K·H has served as a consultant for Eisai and Abbvie. The other authors report no conflicts of interest.

Acknowledgments

We would like to thank Li Huei Tsai (Massachusetts Institute of Technology) for providing access to CamKII-TetOp25 mice. At Sanofi, we also thank Julie Durand, Patrick Juvet, Mati Lopez-Grancha and Nicolas Moindrot for their help during the *in vivo* phase of the pre-clinical studies, Laurent Andrieu for the review of statistical analysis and Catherine Déon for helpful discussion.

Appendix A. Supplementary data

Supplementary data to this article can be found online at https://doi.org/10.1016/j.nbd.2019.104645.

References

Andreasson, U., et al., 2015. A practical guide to immunoassay method validation. Front. Neurol. 6, 179.
Andreasson, U., et al., 2018. Commutability of the certified reference materials for the standardization of beta-amyloid 1-42 assay in human cerebrospinal fluid: lessons for tau and beta-amyloid 1-40 measurements. Clin. Chem. Lab. Med. 56 (12), 2058–2066.
Arendt, T., 2009. Synaptic degeneration in Alzheimer's disease. Acta Neuropathol. 118 (1), 167–179.
Becker, B., et al., 2018. Alzheimer-associated cerebrospinal fluid fragments of neurogranin are generated by Calpain-1 and prolyl endopeptidase. Mol. Neurodegener. 13 (1), 47.
Blanchard, V., et al., 2003. Time sequence of maturation of dystrophic neurites associated with Abeta deposits in APP/PS1 transgenic mice. Exp. Neurol. 184 (1), 247–263.
Blennow, K., et al., 1996. Synaptic pathology in Alzheimer's disease: relation to severity of dementia, but not to senile plaques, neurofibrillary tangles, or the ApoE4 allele. J. Neural Transm. (Vienna) 103 (5), 603–618.
Bogdanovic, N., Davidsson, P., Gottfries, J., Volkna, I., Winblad, B., Blennow, K., 2002. Regional and cellular distribution of synaptic proteins in the normal human brain. Brain Aging 2 (2), 18–30.
Brinkmalm, G., et al., 2012. An online nano-LC-ESI-FTICR-MS method for comprehensive characterization of endogenous fragments from amyloid beta and amyloid precursor protein in human and cat cerebrospinal fluid. J. Mass Spectrom. 47 (5), 591–603.
Brureau, A., et al., 2017. NF-L in cerebrospinal fluid and serum is a biomarker of neuronal damage in an inducible mouse model of neurodegeneration. Neurobiol. Dis. 104, 73–84.
Cruz, J.C., et al., 2003. Aberrant Cdk5 activation by p25 triggers pathological events leading to neurodegeneration and neurofibrillary tangles. Neuron 40 (3), 471–483.
Cruz, J.C., et al., 2006. p25/cyclin-dependent kinase 5 induces production and intraneuronal accumulation of amyloid beta in vivo. J. Neurosci. 26 (41), 10536–10541.
Davidsson, P., Blennow, K., 1998. Neurochemical dissection of synaptic pathology in Alzheimer's disease. Int. Psychogeriatr. 10 (1), 11–23.
Davies, C.A., et al., 1987. A quantitative morphometric analysis of the neuronal and synaptic content of the frontal and temporal cortex in patients with Alzheimer's disease. J. Neurol. Sci. 78 (2), 151–164.
DeKosky, S.T., Scheff, S.W., 1990. Synapse loss in frontal cortex biopsies in Alzheimer's disease: correlation with cognitive severity. Ann. Neurol. 27 (5), 457–464.
DeMattos, R.B., et al., 2002. Plaque-associated disruption of CSF and plasma amyloid-beta (Abeta) equilibrium in a mouse model of Alzheimer's disease. J. Neurochem. 81 (2), 229–236.
Diez-Guerra, F.J., 2010. Neurogranin, a link between calcium/calmodulin and protein kinase C signaling in synaptic plasticity. IUBMB Life 62 (8), 597–606.
Dubois, B., et al., 2014. Advancing research diagnostic criteria for Alzheimer's disease: the IWG-2 criteria. Lancet Neurol. 13 (6), 614–629.
Fischer, A., et al., 2005. Opposing roles of transient and prolonged expression of p25 in synaptic plasticity and hippocampus-dependent memory. Neuron 48 (5), 825–838.
Fischer, A., et al., 2007. Recovery of learning and memory is associated with chromatin remodelling. Nature 447 (7141), 178–182.
Giusti-Rodriguez, P., et al., 2011. Synaptic deficits are rescued in the p25/Cdk5 model of neurodegeneration by the reduction of beta-secretase (BACE1). J. Neurosci. 31 (44), 15751–15756.
Hall, A.M., Roberson, E.D., 2012. Mouse models of Alzheimer's disease. Brain Res. Bull. 88 (1), 3–12.
Henstridge, C.M., Pickett, E., Spires-Jones, T.L., 2016. Synaptic pathology: a shared mechanism in neurological disease. Ageing Res. Rev. 28, 72–84.
Huang, K.P., Huang, F.L., 2011. Calcium-sensitive translocation of calmodulin and neurogranin between Soma and dendrites of mouse hippocampal CA1 neurons. ACS Chem. Neurosci. 2 (4), 223–230.
Huang, K.P., Huang, F.L., Shetty, P.K., 2011. Stimulation-mediated translocation of calmodulin and neurogranin from soma to dendrites of mouse hippocampal CA1 pyramidal neurons. Neuroscience 178, 1–12.
Huber, R.J., Catalano, A., O'Day, D.H., 2013. Cyclin-dependent kinase 5 is a calmodulin-binding protein that associates with puromycin-sensitive aminopeptidase in the nucleus of Dictyostelium. Biochim. Biophys. Acta 1833 (1), 11–20.
Janelidze, S., et al., 2016. CSF Abeta42/Abeta40 and Abeta42/Abeta38 ratios: better diagnostic markers of Alzheimer disease. Ann. Clin. Transl. Neurol. 3 (3), 154–165.
Kester, M.I., et al., 2015. Neurogranin as a cerebrospinal fluid biomarker for synaptic loss in symptomatic Alzheimer disease. JAMA Neurol. 72 (11), 1275–1280.
Kim, D., et al., 2008. Deregulation of HDAC1 by p25/Cdk5 in neurotoxicity. Neuron 60 (5), 803–817.
Kvartsberg, H., et al., 2015. Cerebrospinal fluid levels of the synaptic protein neurogranin correlates with cognitive decline in prodromal Alzheimer's disease. Alzheimers Dement. 11 (10), 1180–1190.
Kvartsberg, H., et al., 2015. Characterization of the postsynaptic protein neurogranin in paired cerebrospinal fluid and plasma samples from Alzheimer's disease patients and healthy controls. Alzheimers Res. Ther. 7 (1), 40.
Kvartsberg, H., et al., 2019. The intact postsynaptic protein neurogranin is reduced in brain tissue from patients with familial and sporadic Alzheimer's disease. Acta Neuropathol. 137, 89–102.
Masliah, E., et al., 2001. Altered expression of synaptic proteins occurs early during progression of Alzheimer's disease. Neurology 56 (1), 127–129.
Mattsson, N., et al., 2016. Cerebrospinal fluid tau, neurogranin, and neurofilament light in Alzheimer's disease. EMBO Mol. Med. 8 (10), 1184–1196.
McKhann, G., et al., 1984. Clinical diagnosis of Alzheimer's disease: report of the NINCDS-ADRDA Work Group under the auspices of Department of Health and Human Services Task Force on Alzheimer's disease. Neurology 34 (7), 939–944.
Mercken, M., et al., 1992. Immunocytochemical detection of the growth-associated protein B-50 by newly characterized monoclonal antibodies in human brain and muscle. J. Neurobiol. 23 (3), 309–321.
Okabe, S., 2007. Molecular anatomy of the postsynaptic density. Mol. Cell. Neurosci. 34 (4), 503–518.
Petersen, A., Gerges, N.Z., 2015. Neurogranin regulates CaM dynamics at dendritic spines. Sci. Rep. 5, 11135.
Portelius, E., et al., 2015. Cerebrospinal fluid neurogranin: relation to cognition and neurodegeneration in Alzheimer's disease. Brain 138 (Pt 11), 3373–3385.
Portelius, E., et al., 2018. Cerebrospinal fluid neurogranin concentration in neurodegeneration: relation to clinical phenotypes and neuropathology. Acta Neuropathol. 136 (3), 363–376.
Rosengren, L.E., et al., 1996. Patients with amyotrophic lateral sclerosis and other neurodegenerative diseases have increased levels of neurofilament protein in CSF. J. Neurochem. 67 (5), 2013–2018.
Savioz, A., Leuba, G., Vallet, P.G., 2014. A framework to understand the variations of PSD-95 expression in brain aging and in Alzheimer's disease. Ageing Res. Rev. 18, 86–94.
Scheff, S.W., et al., 2006. Hippocampal synaptic loss in early Alzheimer's disease and mild cognitive impairment. Neurobiol. Aging 27 (10), 1372–1384.
Scheff, S.W., et al., 2007. Synaptic alterations in CA1 in mild Alzheimer disease and mild cognitive impairment. Neurology 68 (18), 1501–1508.
Scheltens, P., et al., 2016. Alzheimer's disease. Lancet 388 (10043), 505–517.
Schindowski, K., et al., 2006. Alzheimer's disease-like tau neuropathology leads to memory deficits and loss of functional synapses in a novel mutated tau transgenic mouse without any motor deficits. Am. J. Pathol. 169 (2), 599–616.
Serrano-Pozo, A., Froshc, Mp.P., Masliha, E., Hyman, B.T., 2012. Neuropathological alterations in Alzheimer's disease. In: The Biology of Alzheimer's Disease. COld Spring HArbour Laboratory Press, Cold Spring Harbour, NY, pp. 43–65.
Skillback, T., et al., 2014. CSF neurofilament light differs in neurodegenerative diseases and predicts severity and survival. Neurology 83 (21), 1945–1953.
Sundaram, J.R., et al., 2012. Cdk5/p25-induced cytosolic PLA2-mediated lysophosphatidylcholine production regulates neuroinflammation and triggers neurodegeneration. J. Neurosci. 32 (3), 1020–1034.
Sze, C.I., et al., 1997. Loss of the presynaptic vesicle protein synaptophysin in hippocampus correlates with cognitive decline in Alzheimer disease. J. Neuropathol. Exp. Neurol. 56 (8), 933–944.
Thorsell, A., et al., 2010. Neurogranin in cerebrospinal fluid as a marker of synaptic degeneration in Alzheimer's disease. Brain Res. 1362, 13–22.
Wellington, H., et al., 2016. Increased CSF neurogranin concentration is specific to Alzheimer disease. Neurology 86 (9), 829–835.
Willemse, E.A.J., et al., 2018. Neurogranin as cerebrospinal fluid biomarker for Alzheimer disease: an assay comparison study. Clin. Chem. 64 (6), 927–937.